


cambridge.org/mrf

Gui Liu , Chuanba Zhang, Zhuoni Chen and Bo Chen

College of Electrical and Electronic Engineering, Wenzhou University, Wenzhou, China

Research Paper

Cite this article: Liu G, Zhang C, Chen Z, Chen B (2022). A compact dual band MIMO antenna for 5G/WLAN applications. *International Journal of Microwave and Wireless Technologies* **14**, 1347–1352. <https://doi.org/10.1017/S175907872100177X>

Received: 7 April 2021

Revised: 20 December 2021

Accepted: 22 December 2021

First published online: 21 January 2022

Keywords:

MIMO antenna; dual band antenna; 5G; WLAN

Author for correspondence:

Bo Chen, E-mail: chenbo@wzu.edu.cn

Abstract

To satisfy the increasing requirements of wireless communication, a compact dual band MIMO antenna is presented in this paper. The presented antenna consists of two symmetric radiating elements operating at both 3.5 and 4.5 GHz bands. To enhance the isolation between the two radiating elements, an *I*-shaped decoupling structure is introduced. The measured -10 dB reflection coefficients frequency bands are 3.3–3.8 and 4.3–5.8 GHz. The measured isolation S_{21} between the two radiating elements are better than 15 and 17 dB at the lower and higher frequency band, respectively. The overall dimension of the proposed antenna is $50 \times 22 \times 1.59$ mm³. The measured result indicates that the proposed antenna can be a good candidate for 5 G/WLAN wireless communication.

Introduction

Over the past decades, the world has been going through an unprecedented communication revolution, which motivates the development of wireless communication devices. Meanwhile, antenna plays a critical role in wireless communication. With the advent of the 5 G era, there is a soaring demand for multiple-input-multiple-output (MIMO) antennas which have the advantages of high reliability, large gain, and wide bandwidth. More attention, especially in recent years, has been concentrated on the MIMO antenna design.

Two main thorny issues encountered in the design process of MIMO antenna are the gain improvement and the isolation enhancement. In order to address the issues mentioned above, various techniques have been widely studied in recent years. In [1], high isolation between radiating elements has been achieved by placing two elements as mirror symmetrical orientation on different sides of the substrate. A slot on the ground plane was cut to achieve better isolation in [2–4]. Fractal uniplanar compact electromagnetic bandgap (UC-EBG) structure and cross slots were introduced to enhance the isolation [5]. To improve the isolation, grounded stubs and multiple slots are employed in [6–10]. Defected ground structure (DGS) was utilized to reduce the mutual coupling between two antenna elements [11]. Dual band decoupling network was presented to improve the isolation, such as coupled resonators [12] and *T*-sub circuits [13]. Metal vias were placed into the radiating elements in reference [14] to change the excited electromagnetic field distributions, and thus decreased the mutual coupling between two radiating elements effectively.

Moreover, many techniques have been proposed to improve the gain of MIMO antennas [15–19]. In [15], high gain was realized by integrating three pairs of metamaterial (MTM) arrays. Gain can be enhanced by artificial magnetic conductors (AMC) ground plane [16]. Radiating performance has been improved a lot by the *L*-shaped probe array [17]. In [18], an *H*-shaped resonator was used to improve the gain. Two circular slots were applied to increase the gain in [19].

In this paper, a dual-band MIMO antenna operating at both 3.5 and 4.5 GHz frequency bands is proposed. Two radiating elements are printed face to face on a rectangle substrate. Each radiating element includes a *T*-shaped slot and a small *L*-shaped slit. The measured impedance bandwidths of -10 dB reflection coefficients are 500 MHz (3.3–3.8 GHz) and 1500 MHz (4.3–5.8 GHz), and the measured isolation is better than 15 dB.

Antenna design

As shown in Fig. 1, the proposed MIMO antenna is fabricated on a FR4 substrate with ϵ_r of 4.4, $\tan\delta$ of 0.02, and the thickness of 1.59 mm. The proposed antenna consists of two skew symmetry open-loop square radiating elements printed on the top side of the substrate, and two rectangle ground planes with rectangle slot are fabricated on the bottom side of the substrate. Each radiating element contains a *T*-shaped slot and a small *L*-shaped slit. The small *L*-shaped slit mainly resonates at 3.5 GHz band, while the *T*-shaped slot inspires 4.5 GHz band. An *I*-shaped isolation structure with six small rectangle slots (0.5 mm \times 0.3 mm) is applied to decrease the coupling between two elements. And the dimension of each antenna

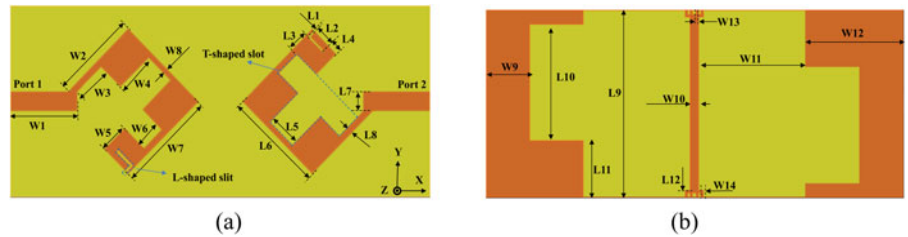


Fig. 1. Configuration of the proposed antenna. (a) top view. (b) bottom view.

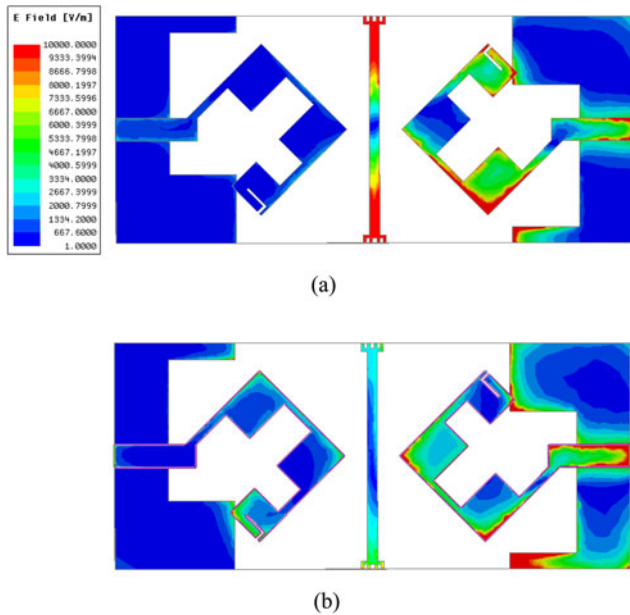


Fig. 2. Simulated E-field distribution at two resonant frequencies. (a) 3.5 GHz. (b) 4.5 GHz.

element is only 11.75 mm × 11.75 mm (0.1754λ₀ × 0.1754λ₀, λ₀ is the free-space wavelength at the frequency of 4.5 GHz).

Parameter analysis

To further understand the principle of the proposed MIMO antenna, the electric field distribution at two resonant frequencies is illustrated in Fig. 2. In Fig. 2(a), the simulated strongest electric field distribution at 3.5 GHz is mainly concentrated at the lower

corner of the radiation element and the isolation structure. The lower intensity of electric field is scattered among the inner upper and right portion of DGS. As shown in Fig. 2(b), the larger intensity of electric field at 4.5 GHz is distributed at the two corners of the radiation element. Therefore, the geometry parameters affecting the proposed MMIO antenna performance can be optimized according to the electric field distribution.

Figure 3 illustrates the simulated S-parameters of the proposed antenna with different value of W8. As can be seen from Fig. 3(a), both resonant frequencies shift toward higher frequencies when the value of W8 becomes larger. As shown in Fig. 3(b), the isolation of the proposed antenna at the higher frequency band is affected by the value of W8. The optimized value of W8 is 0.6 mm.

The optimization of the value of W10 is exhibited in Fig. 4. S₁₁ and S₂₁ parameters almost remain unchanged for the lower frequency band with different value of W10. Therefore, the value of W10 can be effectively used to optimize S₁₁ and S₂₁ parameters of the higher frequency band. The most appropriate value of W10 is 1.0 mm.

Simulation and measurement result

The optimized configuration of the proposed antenna is shown in Table 1. The photograph of the fabricated antenna is presented in Fig. 5.

Figure 6 shows the simulated and measured reflection coefficient. The measured impedance bandwidths of -10 dB reflection coefficients are 500 MHz (3.3–3.8 GHz) and 1500 MHz (4.3–5.8 GHz), respectively. Some deviation of S₁₁ between simulation and measurement is resulted from the soldering process of SMA connectors at the higher frequency band. Therefore, the operating frequency bands of the proposed antenna can cover 5 G New Radio n78 (3.3–3.8 GHz), n79 (4.4–5 GHz) and WLAN (5.15–5.35 GHz) frequency bands. As shown in Fig. 7, the

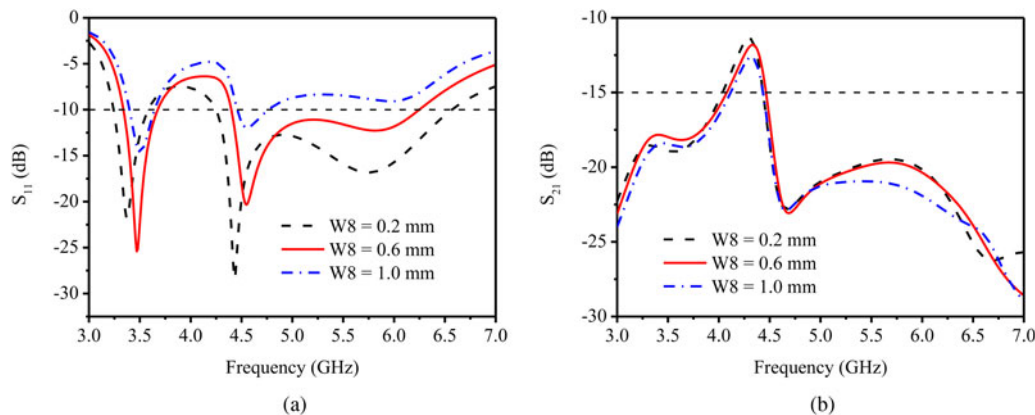


Fig. 3. Simulated S-parameters of the proposed antenna with different value of W8.

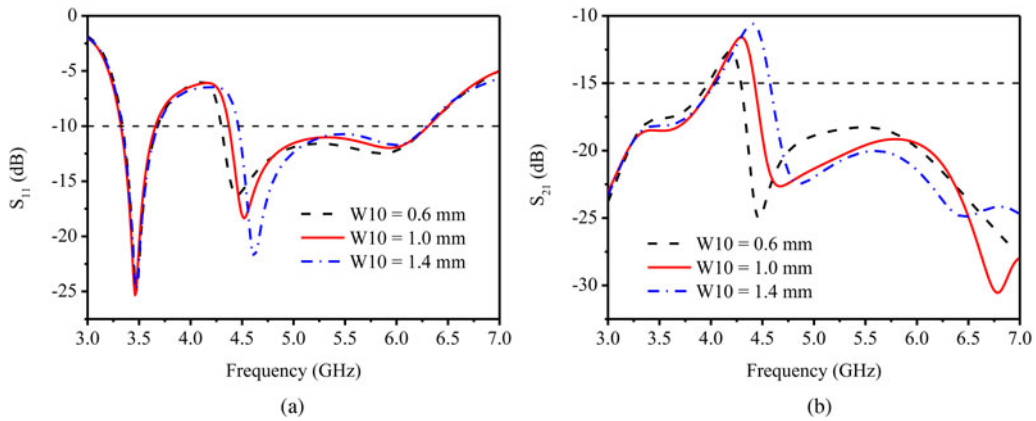


Fig. 4. Simulated S-parameters of the proposed antenna with different value of W10.

Table 1. Parameters of the proposed antenna (in millimetres).

Parameters	W1	W2	W3	W4	W5	W6	W7
Values	7.9	10.2	4.1	4.8	3.4	3.1	11.8
Parameters	W8	W9	W10	W11	W12	W13	W14
Values	0.6	5.2	1.0	12.9	11.7	0.3	0.3
Parameters	L1	L2	L3	L4	L5	L6	L7
Values	0.3	2.3	2.4	1.3	3.8	11.8	2.2
Parameters	L8	L9	L10	L11	L12		
Values	1.8	22.0	13.7	6.7	0.8		

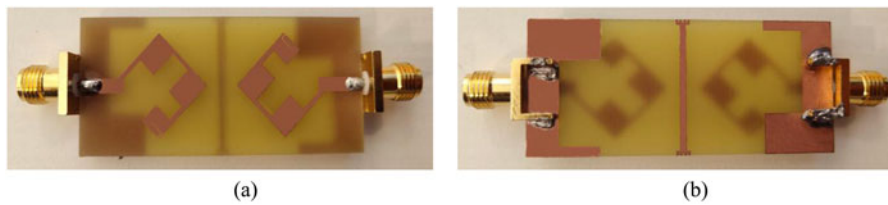


Fig. 5. Photograph of the fabricated antenna. (a) top view. (b) bottom view.

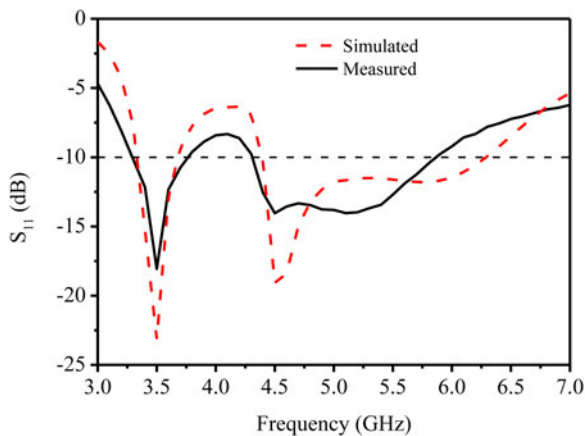


Fig. 6. Simulated and measured reflection coefficients of the proposed antenna.

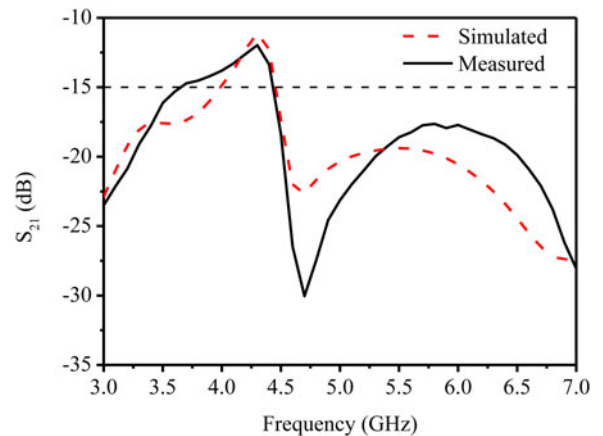


Fig. 7. Simulated and measured isolation of the proposed antenna.

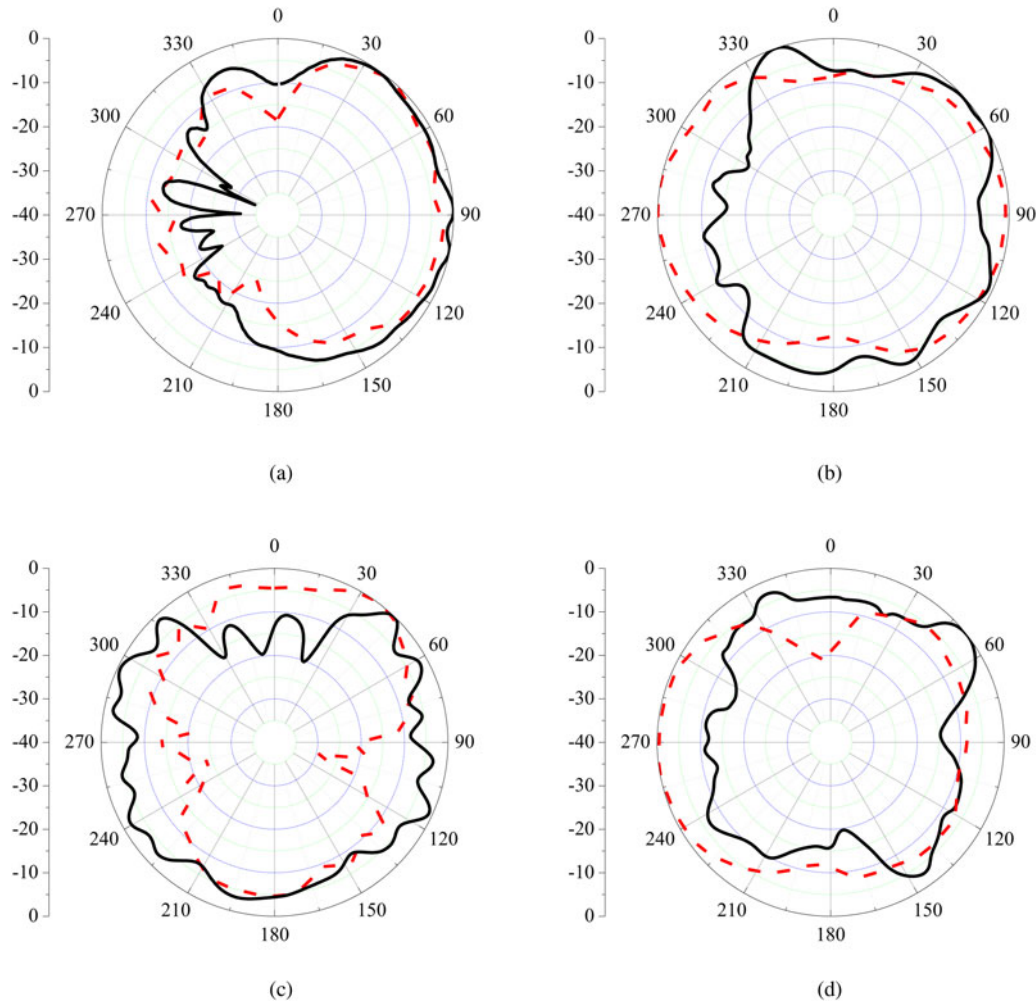


Fig. 8. Measured 2D radiating patterns of the proposed antenna.(a) 3.5 GHz XOY-plane. (b) 3.5 GHz YOZ-plane. (c) 4.5 GHz XOY-plane. (d) 4.5 GHz YOZ-plane.

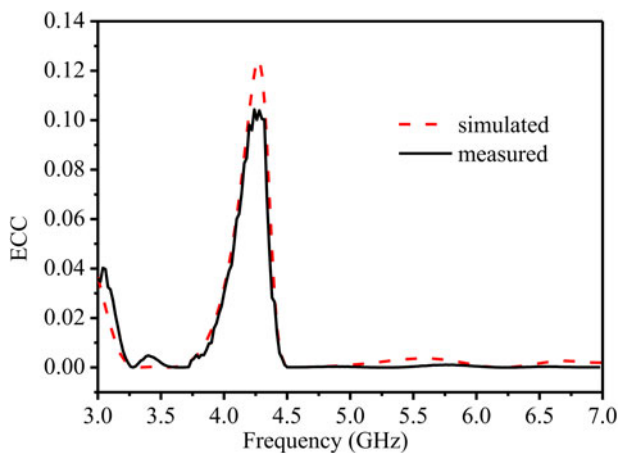


Fig. 9. Simulated and measured ECC of the proposed antenna.

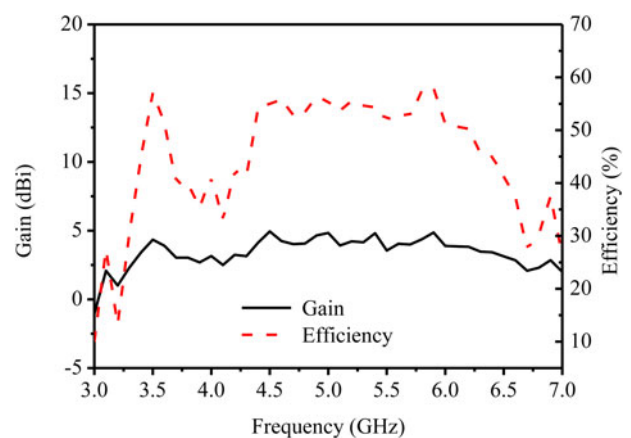


Fig. 10. Gain and efficiency of the proposed antenna.

measured isolations at the lower frequency band and the higher frequency band are better than 15 and 17 dB, respectively. Some divergence between the measured and simulated results occurs due to the fabrication errors and losses.

To further demonstrate the performance of the proposed antenna, Fig. 8 presents the normalized measured antenna

radiating patterns at both 3.5 and 4.5 GHz. Since the presented antenna has a symmetrical structure, port 1 is excited while port 2 is terminated by a $50\ \Omega$ load during the radiating pattern measurement process. As depicted in Fig. 8, the black solid and red dash lines represent co-polarization and cross-polarization, respectively.

Table 2. State-of-the-art of MIMO antenna.

Ref.	−10 dB band (GHz)	Isolation (dB)	ECC	Peak gain (dBi)	Efficiency (%)	Size (mm ³)
This work	3.3–3.8 4.3–5.8	>15 >17	<0.02 <0.015	4.5 5	45 55	50 × 22 × 1.6
[1]	2.32–2.37 3.4–3.62 5.12–5.29	>19 >14 >23	<0.1 <0.1 <0.1	2.81 2.95 2.46	67 75 58	53 × 10.95 × 1.6
[3]	2.4–2.48 5.15–5.83	>15 >13	<0.04 <0.2	/	84	52 × 75 × 1.6
[4]	2.4–2.5 5.1–5.9	>25 >27	<0.01	5 5	45 40	80 × 48 × 0.8
[7]	2.4–2.5 4.9–5.75	>14 >12	<0.014 <0.27	0.5 3.4	50	46 × 20 × 1.6
[8]	2.35–2.53 5.23–5.7	>19.7 >22.98	<0.2 <0.22	4.98 3.34	72 71	75 × 66 × 1

To better demonstrate the MIMO potentials of the presented antenna, ECC was calculated. As one critical standard to assess the performance of MIMO antenna, ECC is a measurement indicator of the correlation level between two radiating elements. The lower ECC is, the better the MIMO performance can be obtained. It is a consensus that the value of ECC must be lower than 0.5 to provide an excellent diversity gain [20]. The ECC between antenna element i and antenna element j can be calculated by the far field pattern as shown in equation (1). The $E_{\theta/\phi, i/j}(\theta, \phi)$ in equation (2) is the θ (or ϕ)-polarized electric far-field patterns of any two antenna elements in a spherical coordinate.

$$\rho_{ij} = \frac{\iint_{4\pi} A_{ij}(\theta, \phi) \sin(\theta) d\theta d\phi}{\sqrt{\iint_{4\pi} A_{ii}(\theta, \phi) \sin(\theta) d\theta d\phi} \sqrt{\iint_{4\pi} A_{jj}(\theta, \phi) \sin(\theta) d\theta d\phi}} \quad (1)$$

where:

$$A_{ij}(\theta, \phi) = E_{\theta, i}(\theta, \phi) E_{\theta, j}^*(\theta, \phi) + E_{\phi, i}(\theta, \phi) E_{\phi, j}^*(\theta, \phi) \quad (2)$$

Moreover, ECC can also be estimated by the following equation (3):

$$\rho_{ij} = \frac{|S_{ii}^* S_{ij} + S_{ji}^* S_{jj}|^2}{(1 - (|S_{ii}|^2 + |S_{jj}|^2))(1 - (|S_{ij}|^2 + |S_{ji}|^2))} \quad (3)$$

where S_{ii} is the reflection coefficient of antenna element i , and S_{ij} ($i \neq j$) represents the transmission coefficient between two antenna elements. Equation (3) can be used only under some assumptions such as a lossless antenna in a rich isotropic multipath (RIMP) scenario. Equation (3) is selected to make a rough estimation of ECC. The real and imaginary part of both S_{11} and S_{21} were measured by the Vector Network Analyser (VNA) N5224A. Since the proposed antenna has a quiet symmetrical structure, only Port 1 is measured. The calculated ECC of the antenna is depicted in Fig. 9. The calculated ECCs of the antenna are below 0.02 in both operating bands, which is far smaller than 0.5.

In Fig. 10, the peak gain and radiating efficiency were illustrated. The measured peak gain of the proposed antenna is nearly 4.5 and 5 dBi at 3.3–3.8 GHz and 4.3–5.8 GHz frequency bands, respectively. The measured efficiency is better than 55% in both operating bands. A performance comparison between the

proposed antenna with state-of-the-art 5G/WLAN MIMO antennas is depicted in Table 2. The main contribution of our work is that we propose a dual-band 5G/WLAN MIMO antenna with lower ECC, smaller size and wider frequency bandwidths.

Conclusion

This paper presents a compact dual-band MIMO antenna for 5G/WLAN applications. The measured −10 dB bandwidth are 500 MHz (3.3–3.8 GHz) and 1500 MHz (4.3–5.8 GHz), which can cover the 5G New Radio n78 (3.3–3.8 GHz), n79 (4.4–5 GHz) and WLAN (5.15–5.35 GHz) frequency bands. The measured isolation between two radiating elements is better than 15 and 17 dB at both operating frequency bands, respectively. The proposed antenna has a peak gain of 4.5 dBi at the lower frequency band and 5 dBi at the higher frequency band, respectively. The measured efficiency is almost 55% and the measured ECC values are smaller than 0.02 in both operating bands. Therefore, the presented antenna can be regarded as a good candidate for 5G/WLAN mobile terminals.

Acknowledgements. This work was funded in part by the National Natural Science Foundation of China under Grant No. 61671330, the Science and Technology Department of Zhejiang Province under Grant No. LGG19F010009, and Wenzhou Municipal Science and Technology Program under Grant No. C20170005 and No.2018ZG019.

References

1. You X, Gao H, Zhou L and Zhao H (2015) Compact dual-element inverted-F MIMO antenna system with enhanced isolation. *Microwave and Optical Technology Letters* **58**, 363–368.
2. Huang J, Dong G, Cai J, Li H and Liu G (2021) A quad-port dual-band MIMO antenna array for 5G smartphone applications. *Electronics* **10**, 542–550.
3. Deng J, Li J, Zhao L and Guo L (2017) A dual-band inverted-F MIMO antenna with enhanced isolation for WLAN applications. *IEEE Antennas and Wireless Propagation Letters* **16**, 2270–2273.
4. Shen DL, Zhang L, Jiao YC and Yan YD (2019) Dual-element antenna with high isolation operating at the WLAN bands. *Microwave and Optical Technology Letters* **61**, 2323–2328.
5. Yang X, Liu Y, Xu Y and Gong S (2017) Isolation enhancement in patch antenna array with fractal UC-EBG structure and cross slot. *IEEE Antennas and Wireless Propagation Letters* **16**, 2175–2178.

6. **Lee J, Kim S and Jang J** (2015) Reduction of mutual coupling in planar multiple antenna by using 1-D EBG and SRR structures. *IEEE Transactions on Antennas and Propagation* **63**, 4194–4198.
7. **Soltani S, Lotfi P and Murch RD** (2017) A dual-band multiport MIMO slot antenna for WLAN applications. *IEEE Antennas and Wireless Propagation Letters* **16**, 529–532.
8. **Fang HS, Wu CY, Sun JS and Huang JT** (2017) Design of a compact MIMO antenna with pattern diversity for WLAN application. *Microwave and Optical Technology Letters* **59**, 1692–1697.
9. **Ren Z and Zhao A** (2019) Dual-band MIMO antenna with compact self-decoupled antenna pairs for 5 G mobile applications. *IEEE Access* **7**, 82288–82296.
10. **Chen Q, Lin H, Wang J, Ge L, Li Y, Per T and Sim C** (2018) Single ring slot-based antennas for metal-rimmed 4G/5G smartphones. *IEEE Transactions on Antennas and Propagation* **67**, 1476–1487.
11. **Kim S and Choi J** (2018) Two-port UWB MIMO antenna with modified ground for isolation improvement. 2018 *International Symposium on Antennas and Propagation (ISAP)*, pp. 1–2.
12. **Zhao L and Wu K** (2015) A dual-band coupled resonator decoupling network for two coupled antennas. *IEEE Transactions on Antennas and Propagation* **63**, 2843–2850.
13. **Sui J and Wu K** (2017) A general T-stub circuit for decoupling of two dual-band antennas. *IEEE Transactions on Microwave Theory and Techniques* **65**, 2111–2121.
14. **Pan YM, Qin X, Sun YX and Zheng SY** (2019) A simple decoupling method for 5 G millimetre-wave MIMO dielectric resonator antennas. *IEEE Transactions on Antennas and Propagation* **67**, 2224–2234.
15. **Jiang H, Si L, Hu W and Lv X** (2019) A symmetrical dual-beam bowtie antenna with gain enhancement using metamaterial for 5 G MIMO applications. *IEEE Photonics Journal* **11**, 1–9.
16. **Yang W, Wang H, Che W and Wang J** (2013) A wideband and high-gain edge-zeeed patch antenna and array using artificial magnetic conductor structures. *IEEE Antennas and Wireless Propagation Letters* **12**, 769–772.
17. **Wang L, Guo Y and Sheng W** (2012) A 60-GHz wideband L-probe patch antenna array with gain enhanced structure based on LTCC technology. *2012 Asia Pacific Microwave Conference Proceedings*, pp. 151–153.
18. **Wang H, Liu S, Chen L, Li W and Shi X** (2014) Gain enhancement for broadband vertical planar printed antenna with H-shaped resonator structures. *IEEE Transactions on Antennas and Propagation* **62**, 4411–4415.
19. **Squadrito P, Zhang S and Pedersen GF** (2019) X-band antenna with enhanced gain and sidelobe suppression. *13th European Conference on Antennas and Propagation (EuCAP)*, Krakow, Poland, pp. 1–4.
20. **Vaughan R and Andersen J** (1987) Antenna diversity in mobile communications. *IEEE Transactions on Vehicular Technology* **36**, 149–172.



Gui Liu received his B.S. degree from South China University of Technology in 1997, the M.S. degree from Sun Yat-sen University in 2003, and the Ph.D. degree from Illinois Institute of Technology in 2011. He is currently a professor of Wenzhou University, Wenzhou, China. His research interests include RF integrated circuit design, microwave device and antenna design.



Chuanba Zhang received the B.S. degree from Nan Yang Institute of Technology in 2019, he is currently pursuing his M.S. degree in Wenzhou University. His current research interests include RF integrated circuit design and antenna design.



Zhuoni Chen received her B.S. degree from Guangdong Ocean University in 2020. She is currently pursuing her M.S. degree in Wenzhou University. Her research interests include RF integrated circuit design and antenna design.



Bo Chen received the B.S. degree in microelectronics from Peking University and the M.S. degree in microelectronics and solid-state electronics from institute of microelectronics of the Chinese Academy of Science, Beijing, China. He is currently an assistant professor in Wenzhou University, Wenzhou, China. His research interesting includes hardware security, hardware obfuscation, and antenna design.